Title

The Resolution of Chiral, Tetrahedral M4L6 Metal-Ligand Hosts

Authors

Davis, Anna V.
Fiedler, Dorothea
Ziegler, Marco
et al.

Publication Date

2007-08-28

The Resolution of Chiral, Tetrahedral M_4L_6 Metal-Ligand Hosts

Anna V. Davis, Dorothea Fiedler, Marco Ziegler, Andreas Terpin, and Kenneth N. Raymond

Department of Chemistry, University of California, Berkeley, CA 94720-1460
and
Lawrence Berkeley National Laboratory, Berkeley, CA 94720

ABSTRACT The supramolecular metal-ligand assemblies of $M_4\mathbf{1}_6$ stoichiometry are chiral (M = Ga^{III}, Al^{III}, In^{III}, Fe^{III}, Ti^{IV}, or Ge^{IV}, $H_4\mathbf{1}$ = *N,N′-bis*(2,3-dihydroxybenzoyl)-1,5-diaminonaphthalene). The resolution process of $\Delta\Delta\Delta\Delta$- and $\Lambda\Lambda\Lambda\Lambda$-$[M_4\mathbf{1}_6]^{12-}$ by the chiral cation s-nicotinium (*S*-nic$^+$) is described for the Ga^{III}, Al^{III}, and Fe^{III} assemblies, and the resolution is shown to be proton dependent. From a methanol solution of $M(acac)_3$, $H_4\mathbf{1}$, *S*-nicI, and KOH, the $\Delta\Delta\Delta\Delta$-KH_3(*S*-nic)$_7$[(*S*-nic) $\subset$ $M_4\mathbf{1}_6$] complexes precipitate, and the $\Lambda\Lambda\Lambda\Lambda$-$K_6$(*S*-nic)$_5$[(*S*-nic) $\subset$ $M_4\mathbf{1}_6$] complexes subsequently can be isolated from the supernatant. Ion exchange enables the isolation of the $(NEt_4^+)_{12}$, $(NMe_4^+)_{12}$ and K^+_{12} salts of the resolved structures, which have been characterized by CD and NMR spectroscopies. Resolution can also be accomplished with one equivalent of NEt_4^+ blocking the cavity interior, demonstrating that external binding sites are responsible for the difference in *S*-nic$^+$ enantiomer interactions. Circular dichroism data demonstrate that the $(NMe_4^+)_{12}$ and $(NEt_4^+)_{12}$ salts of the resolved $[Ga_4\mathbf{1}_6]^{12-}$ and $[Al_4\mathbf{1}_6]^{12-}$ structures retain their chirality over extended periods of time (>20 d) at room temperature; heating the $(NEt_4^+)_{12}[Ga_4\mathbf{1}_6]$ assembly to 75 °C also had no effect on its CD spectrum. Finally, experiments with the resolved $K_{12}[Ga_4\mathbf{1}_6]$ assemblies point to the role of a guest in stabilizing the resolved framework.

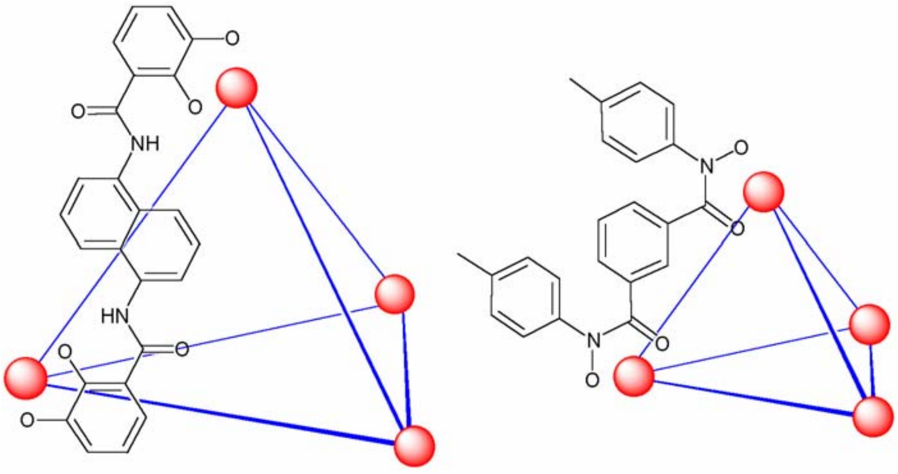

Figure 1. Schematic representations of the $M_4\mathbf{1}_6$ (left) and $M_4\mathbf{2}_6$ (right) tetrahedra.

J. Am Chem. Soc. **2007,** *129*, 15354-15363

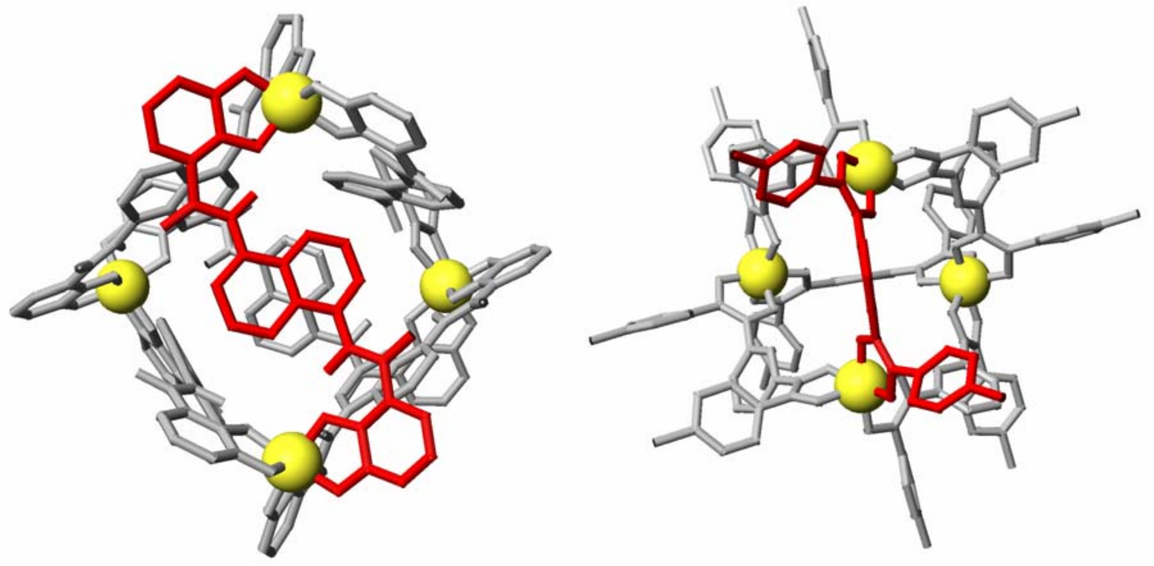

Figure 2. Crystal structures of $[Fe_4\mathbf{1}_6]^{12-}$ and $[Ga_4\mathbf{2}_6]$.[10, 21] The C_2 axis is perpendicular to the ligand backbone of **1** but is in the plane of the ligand backbone of **2**.

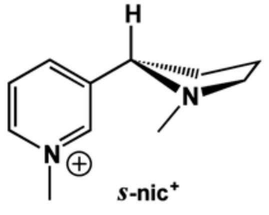

Figure 3. Chiral (*S*)-*N*-methyl-nicotinium (*S*-nic$^+$) cation used in $[M_4\mathbf{1}_6]^{12-}$ resolution.

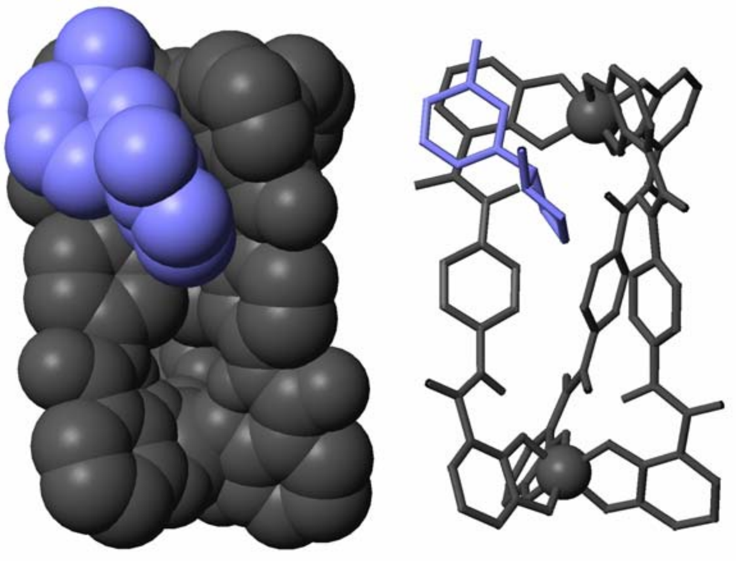

Figure 4. Space filling (left) and cylinder (right) representations of the crystal structure of *ΛΛ*-K(*S*-nic)$_5$[Ga$_2$**3**$_3$]. For simplicity, only one *S*-nic$^+$ counter ion is included.[14]

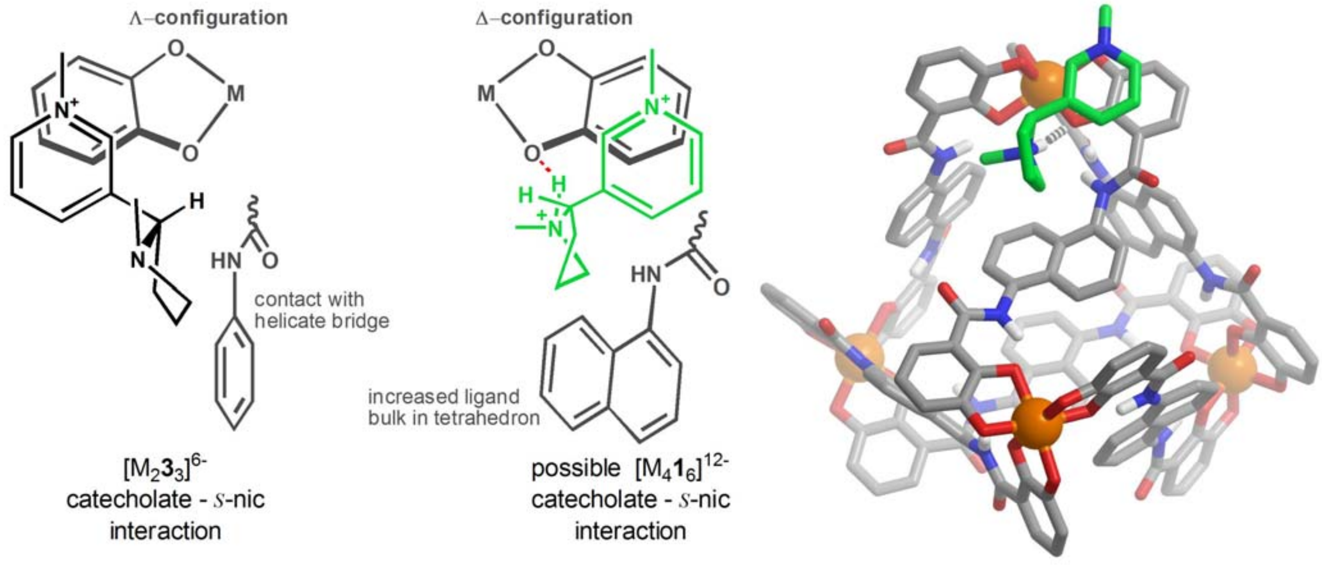

Figure 5. Left: simplified representation of the *S*-nic$^+$-[M$_2$**3**$_3$]$^{6-}$ helicate interaction. Middle: proposed *S*-nic$^+$ interaction with the [M$_4$**1**$_6$]$^{12-}$ tetrahedron which might account for pyrrolidine protonation and the differences between the steric demands of the helicate and tetrahedron ligands. A pyrrolidinium-catecholate hydrogen bond is highlighted in red. Right: Modeled *S*-nicH^{2+}–[M$_4$**1**$_6$]$^{12-}$ interaction (CAChe, MM3)[27], carbons of the *S*-nicH^{2+} cation are shown in green for clarity.

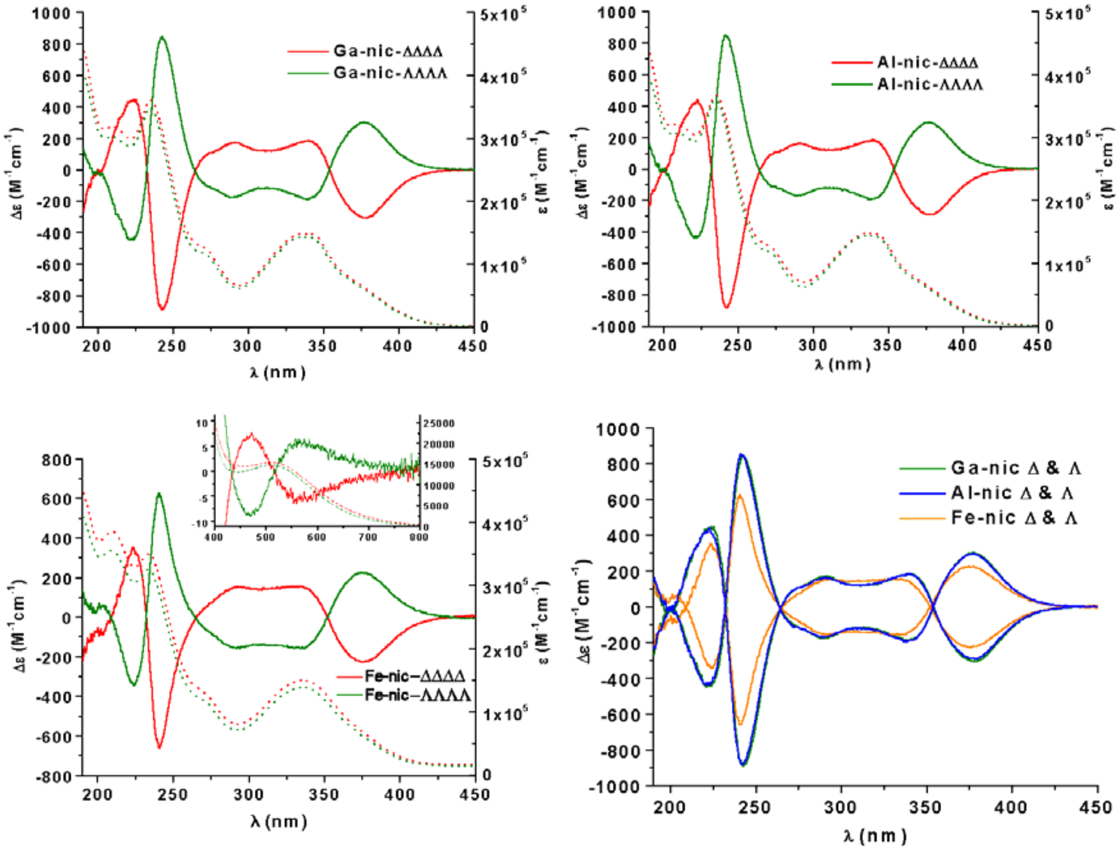

Figure 6. CD (solid lines) and UV-Vis (dotted lines) spectra of the *S*-nic$^+$ salts of the resolved [Ga$_4$**1**$_6$]$^{12-}$, [Al$_4$**5**$_6$]$^{12-}$, and [Fe$_4$**5**$_6$]$^{12-}$ tetrahedral assemblies.

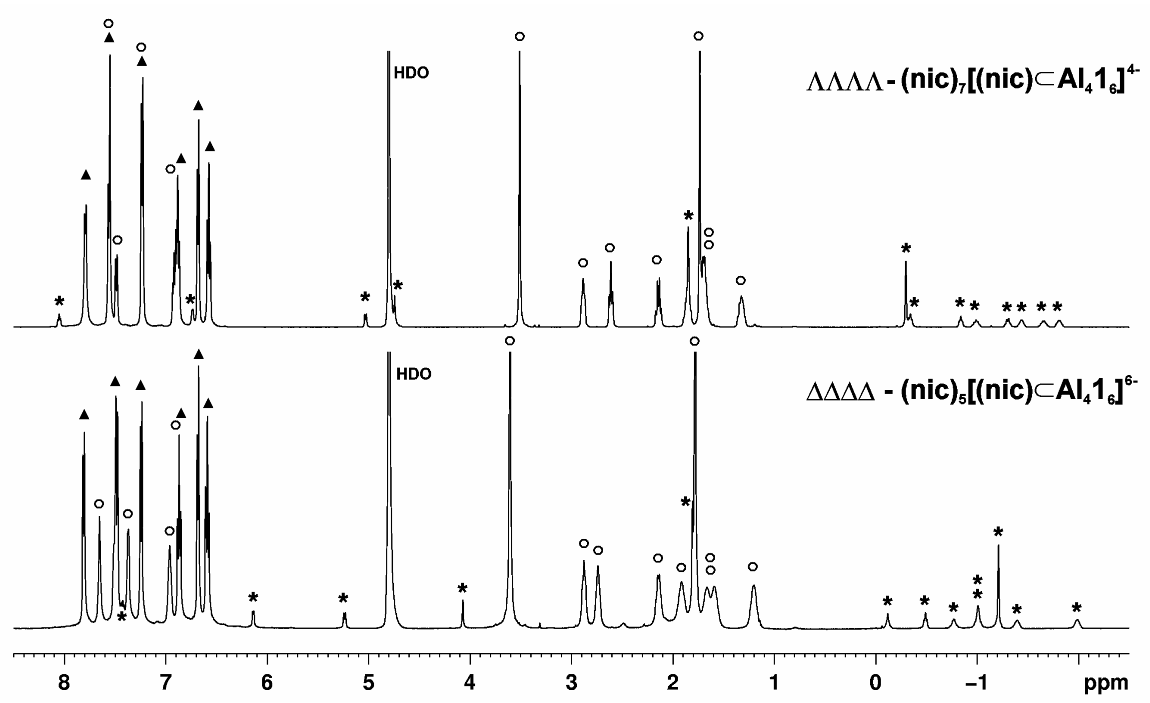

Figure 7. ^{1}H NMR (500 MHz, D_2O) spectra of the *ΛΛΛΛ*-(*S*-nic)$_7$[(*S*-nic) ⊂ Al_4**1**$_6$]$^{4-}$ and *ΔΔΔΔ*-(*S*-nic)$_5$ [(*S*-nic) ⊂ Al_4**1**$_6$]$^{6-}$ complexes. (▲ = host; o = exterior *S*-nic$^+$; * = encapsulated *S*-nic$^+$)

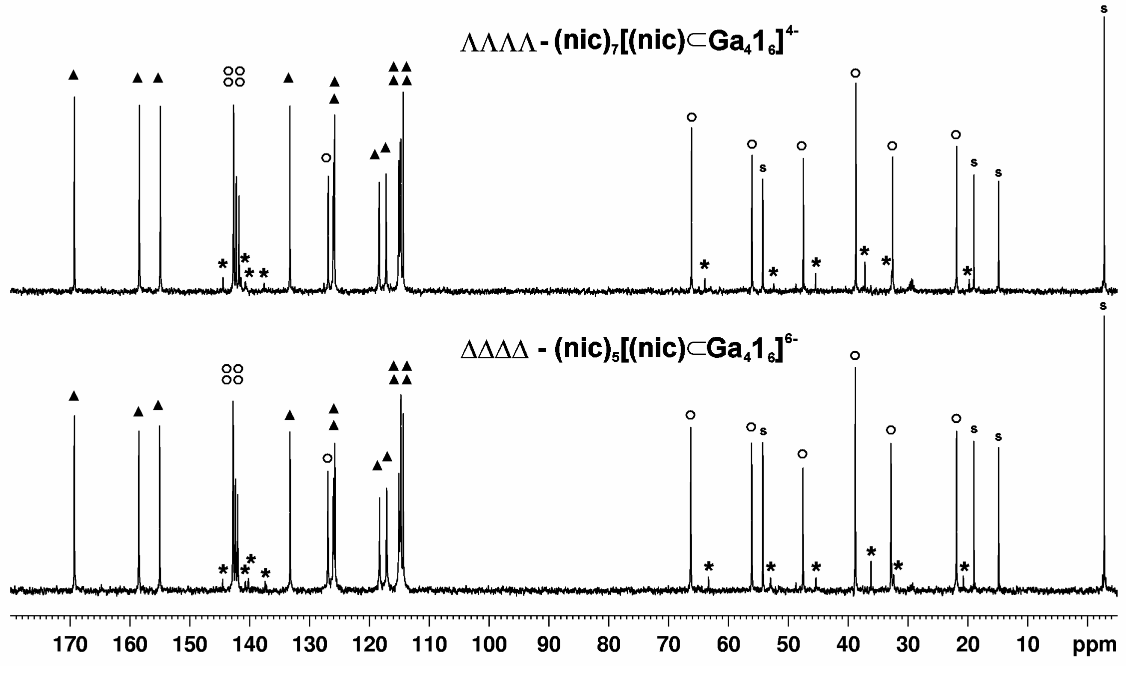

Figure 8. ^{13}C NMR (100 MHz, D_2O) spectra of *ΛΛΛΛ*-(*S*-nic$^+$)$_7$[(*S*-nic$^+$) ⊂ Ga_4**1**$_6$]$^{4-}$ and *ΔΔΔΔ*-(*S*-nic)$_5$ [(*S*-nic) ⊂ Ga_4**1**$_6$]$^{6-}$. (▲ = host; o = exterior *S*-nic$^+$; * = encapsulated *S*-nic$^+$, s = internal standard)

Table 1. ^{1}H NMR data for *S*-nic$^+$ [$M_4\mathbf{1}_6$]$^{12-}$ compounds. (500 MHz, D_2O)

^{1}H NMR	**Ga ΔΔΔΔ**	**Ga ΛΛΛΛ**	**Al ΔΔΔΔ**	**Al ΛΛΛΛ**
Host Ar(H)				
naphthyl-*H*	7.81 (d, *J* = 7.6, 12H)	7.79 (d, *J* = 7.5, 12H)	7.81 (d, *J* = 7.6, 12H)	7.79 (d, *J* = 7.0, 12H)
naphthyl-*H*	7.49 (d, *J* = 8.4, 12H)	7.55 (d, *J* = 8.5, 12H)	7.48 (d, *J* = 8.7, 12H)	7.56 (d, *J* = 8.7, 12H)
catechol-*H*	7.28 (d, *J* = 8.4, 12H)	7.27 (d, *J* = 8.4, 12H)	7.24 (d, *J* = 8.2, 12H)	7.23 (d, *J* = 7.6, 12H)
naphthyl-*H*	6.84 (t, *J* = 8.0, 12H)	6.85 (t, *J* = 7.9, 12H)	6.86 (t, *J* = 8.0, 12H)	6.88 (t, *J* = 7.4, 12H)
catechol-*H*	6.75 (d, *J* = 7.3, 12H)	6.76 (d, *J* = 7.3, 12H)	6.68 (d, *J* = 7.3, 12H)	6.68 (d, *J* = 7.1, 12H)
catechol-*H*	6.59 (t, *J* = 7.6, 12H)	6.58 (t, *J* = 7.3, 12H)	6.59 (t, *J* = 8.0, 12H)	6.58 (t, *J* = 7.3, 12H)
***S*-nic$^+$ (exterior)**				
pyridinium-*H*	7.67 (s, 7H)	7.56 (s, 5H)	7.65 (s, 7H)	7.55 (s, 5H)
pyridinium-*H*	7.53 (d, *J* = 7.9, 7H)	7.50 (d, *J* = 8.0, 5H)	7.49 (br m, 7H)	7.50 (d, *J* = 8.0, 5H)
pyridinium-*H*	7.42 (d, *J* = 5.2, 7H)	7.29 (d, *J* = n.d., 5H)	7.36 (br m, 7H)	7.23 (d, *J* = n.d., 5H)
pyridinium-*H*	6.97 (t, *J* = 6.6, 7H)	6.94 (t, *J* = 6.8, 5H)	6.96 (br m, 7H)	6.92 (t, *J* = 6.5, 5H)
pyridinium-NCH_3	3.61 (s, 21H)	3.51 (s, 15H)	3.61 (s, 21H)	3.51 (s, 15H)
pyrrolidine-*H*	2.88 (t, *J* = 8.3, 7H)	2.88 (br m, 5H)	2.88 (br m, 7H)	2.88 (br m, 5H)
pyrrolidine-*H*	2.75 (t, *J* = 8.1, 7H)	2.60 (t, *J* = 8.3, 5H)	2.74 (br m, 7H)	2.61 (t, *J* = 8.1, 5H)
pyrrolidine-*H*	2.14 (q, *J* = 9.0, 7H)	2.13 (q, *J* = 8.9, 5H)	2.14 (br m, 7H)	2.14 (q, *J* = 8.7, 5H)
pyrrolidine-*H*	1.92 (br m, 7H)	1.82 (br m, 5H)	1.91 (br m, 7H)	1.86 (br m, 5H)
pyrrolidine-NCH_3	1.79 (s, 21H)	1.73 (s, 15H)	1.78 (s, 21H)	1.73 (s, 15H)
pyrrolidine-*H*	1.66 (br m, 7H)	1.69 (br m, 10H)	1.66 (br m, 7H)	1.69 (br m, 10H)
pyrrolidine-*H*	1.59 (br m, 7H)	1.32 (br m, 5H)	1.59 (br m, 7H)	1.33 (br m, 5H)
pyrrolidine-*H*	1.20(br m, 7H)		1.20(br m, 7H)	
***S*-nic$^+$ (encapsulated)**				
pyridinium-*H*	7.35 (t, *J* = 6.2, 1H)	7.93 (t, *J* = 6.2, 1H)	7.42 (t, *J* = 6.9, 1H)	8.05 (t, *J* = 6.20, 1H)
pyridinium-*H*	6.16 (d, *J* = 4.9, 1H)	6.71 (d, *J* = 5.2, 1H)	6.14 (t, *J* = 5.1, 1H)	6.73 (d, *J* = 5.0, 1H)
pyridinium-*H*	5.23 (d, *J* = 7.6, 1H)	5.02 (d, *J* = 7.7, 1H)	5.24 (d, *J* = 7.8, 1H)	5.03 (d, *J* = 7.9, 1H)
pyridinium-*H*	4.11 (s,1H)	4.72 (s,1H)	4.07 (s, 1H)	4.74 (s,1H)
pyridinium-NCH_3	1.81 (s, 3H)	1.83 (s, 3H)	1.81 (s, 3H)	1.85 (s, 3H)
pyrrolidine-*H*	-0.07 (br m, 1H)	-0.34 (br m, 1H)	-0.12 (br m, 1H)	-0.30 (s, 3H)
pyrrolidine-*H*	-0.47 (t, *J* = 7.2, 1H)	-0.37 (s, 3H)	-0.49 (t, *J* = 7.7, 1H)	-0.34 (t, *J* = 7.3, 1H)
pyrrolidine-*H*	-0.76 (br m, 1H)	-0.77 (br m, 1H)	-0.77 (br m, 1H)	-0.84 (br m, 1H)
pyrrolidine-*H*	-0.97 (br m, 2H)	-0.98 (br m, 1H)	-1.01 (br m, 2H)	-0.99 (br m, 1H)
pyrrolidine- NCH_3	-1.16 (s, 3H)	-1.27 (br m, 1H)	-1.21 (s, 3H)	-1.14 (br m, 1H)
pyrrolidine-*H*	-1.34 (br m, 1H)	-1.40 (br m, 1H)	-1.39 (br m, 1H)	-1.30 (br m, 1H)
pyrrolidine-*H*	-1.96 (br m, 1H)	-1.62 (br m, 1H)	-1.99 (br m, 1H)	-1.66 (br m, 1H)
pyrrolidine-*H*		-1.81 (br m, 1H)		-1.81 (br m, 1H)

^{1}H Chemical shifts are referenced to a sodium 3-(trimethylsilyl)-propane sulfonate internal standard.

Table 2. ^{13}C NMR data for *S*-nic$^+$ [M_4**1**$_6$]$^{12-}$ compounds. (100 MHz, D_2O)

^{13}C NMR	**Ga** ΔΔΔΔ	**Ga** ΛΛΛΛ	**Al** ΔΔΔΔ	**Al** ΛΛΛΛ
Host				
carbonyl-*CO*	170.0	170.0	170.0	170.0
catechol-*CO*	159.2	159.1	160.2	160.1
catechol-*CO*	155.7	155.6	156.9	156.7
catechol-*C*	134.0	134.0	134.0	134.0
catechol-*C*	126.8	126.8	126.7	126.7
catechol-*C*	126.5	126.6	126.5	126.6
naphthyl-*C*	119.1	119.1	119.1	119.3
naphthyl-*C*	117.9	118.0	117.9	118.0
naphthyl-*C*	115.8	115.9	115.7	115.7
naphthyl-*C*	115.7	115.6	115.5	115.5
naphthyl-*C*	115.5	115.5	114.7	114.8
Naphthyl-*C*	115.1	115.5	114.6	114.6
***S*-nic$^+$ (ext)**				
pyrid.-*C*	143.6	143.5	143.5	143.4
pyrid.-*C*	143.4	143.4	143.4	143.2
pyrid.-*C*	143.1	143.0	143.2	142.9
pyrid.-*C*	142.8	142.5	142.8	142.5
pyrid.-*C*	127.7	127.7	127.7	127.6
pyrid.-NCH_3	67.1	66.9	67.1	66.9
pyrol.-*C*	56.9	56.8	56.9	56.8
pyrol.-*C*	48.3	48.2	48.3	48.3
pyrol.-NCH_3	39.6	39.4	39.6	39.5
pyrol.-*C*	33.6	33.3	33.6	33.3
pyrol.-*C*	22.7	22.6	22.7	22.6
***S*-nic$^+$ (enc.)**				
pyrid.-*C*	145.3	145.2	145.2	145.2
pyrid.-*C*	142.7	142.2	142.7	142.3
pyrid.-*C*	141.5	141.5	140.9	141.5
pyrid.-*C*	141.0	138.4	138.1	138.3
pyrid.-*C*	127.6	128.4	128.2	128.6
pyrid.-NCH_3	64.1	64.7	64.0	64.6
pyrol.-*C*	53.7	53.2	53.7	53.1
pyrol.-*C*	46.1	46.2	46.1	46.2
pyrol.-NCH_3	37.0	37.9	37.0	38.2
pyrol.-*C*	33.1	33.4	33.0	33.5
pyrol.-*C*	21.5	20.6	21.6	20.6

^{13}C Chemical shifts are referenced to a sodium 3-(trimethylsilyl)-propane sulfonate internal standard.

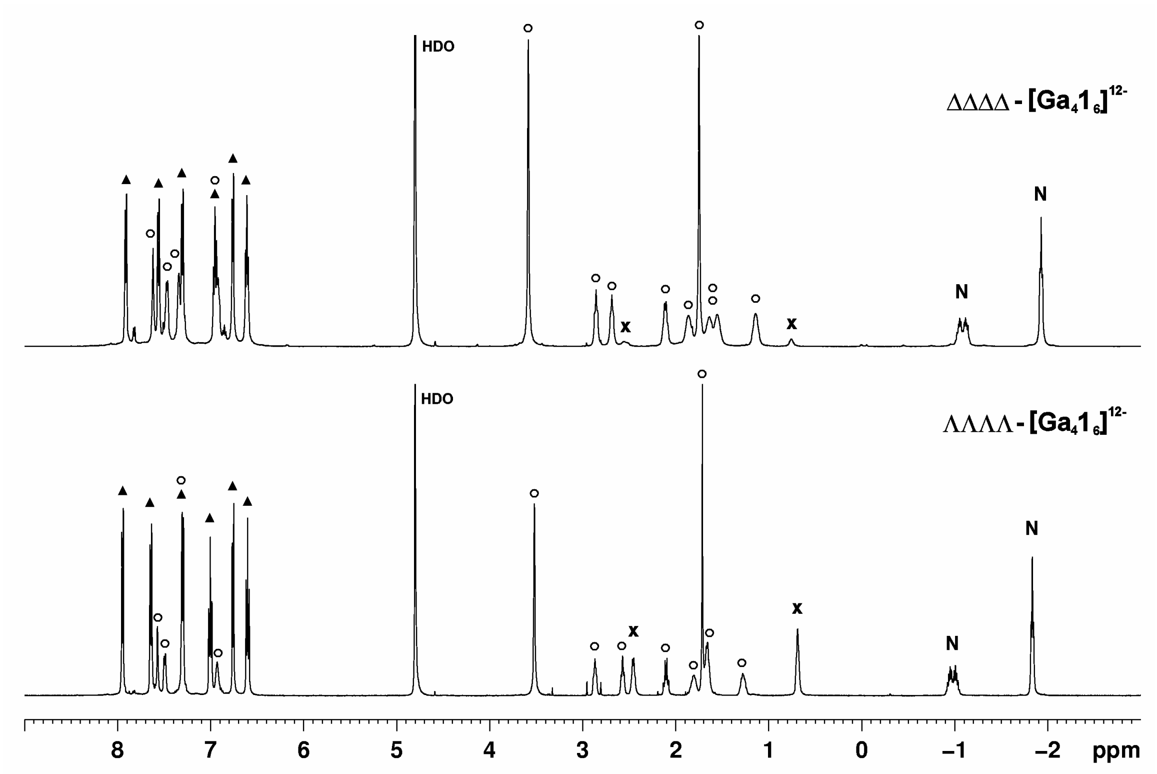

Figure 9. ^{1}H NMR (500 MHz, D_2O) of the *S*-nic^{+} salts of the resolved $[(NEt_4)\subset Ga_4\mathbf{1}_6]^{11-}$ enantiomers. (▲ = host; o = exterior *S*-nic^{+}; N = encapsulated NEt_4^{+}, x = external NEt_4^{+})

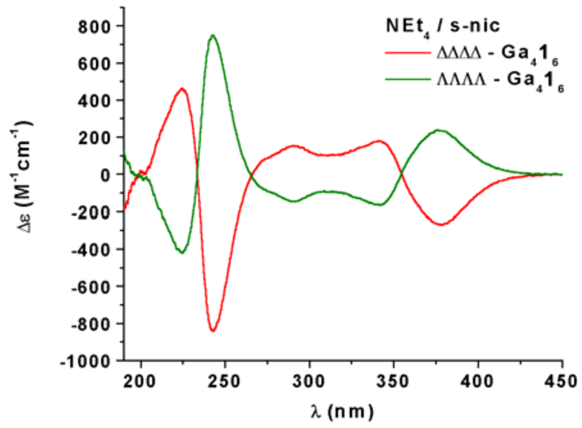

Figure 10. CD spectra of the *S*-nic^{+} salts of the resolved $[(NEt_4)\subset Ga_4\mathbf{1}_6]^{11-}$ enantiomers.

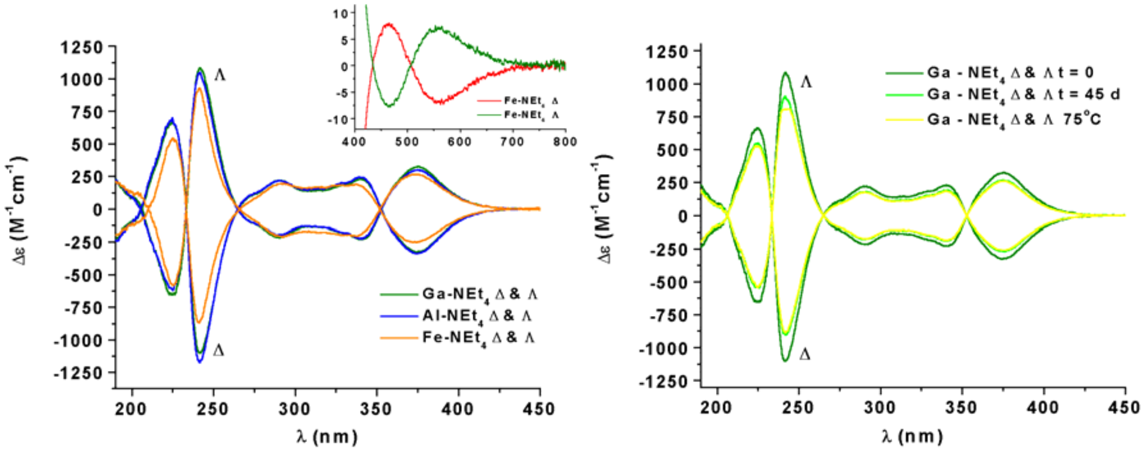

Figure 11. Left: CD spectra of the NEt$_4^+$ salts of the *ΔΔΔΔ*- and *ΛΛΛΛ*- enantiomers of $[\mathrm{Ga}_4\mathbf{1}_6]^{12-}$, $[\mathrm{Al}_4\mathbf{1}_6]^{12-}$ and $[\mathrm{Fe}_4\mathbf{1}_6]^{12-}$. Right: CD spectra of the Ga$^{\mathrm{III}}$ compounds taken immediately after preparation of the 0.5 mM solution, after 45 days, and then after 24 h of heating to 75 °C.

Table 3. Summary of $[\mathrm{M}_4\mathbf{1}_6]^{12-}$ CD data

Complex	**Ga$^{\mathrm{III}}$**	**Al$^{\mathrm{III}}$**	**Fe$^{\mathrm{III}}$**
ΔΔΔΔ-$(S\text{-nic})_6[\mathrm{M}_4\mathbf{1}_6]^{6-}$	225 (+448); 242 (-889); 291 (+173); 340 (+187), 379 (-306)	223 (+443); 242 (-883); 290 (+165); 339 (+187); 378 (-292)	223 (+356); 241 (-659); 292 (+155); 339 (+146); 376 (+228); 468 (+7); 565 (-6)
ΛΛΛΛ-$(S\text{-nic})_8[\mathrm{M}_4\mathbf{1}_6]^{4-}$	221 (-448); 243 (+848); 288 (-177); 339 (-190); 377 (+304)	221 (-437); 241 (+854); 288 (-170); 337 (-194); 377 (+298)	224 (-344); 241 (+627); 292 (-157); 337 (-159); 375 (+228); 468 (-8); 565 (+6)
ΔΔΔΔ-$(\mathrm{NEt}_4)_{12}[\mathrm{M}_4\mathbf{1}_6]$	225 (+664); 241 (-1102); 290 (+223); 340 (+230); 375 (-329)	225 (+701); 242 (-1173); 290 (+219); 339 (245); 375 (-339)	225 (+544); 241 (-869); 293 (+198); 337 (+191); 374 (-253); 465 (8); 560 (-7)
ΛΛΛΛ-$(\mathrm{NEt}_4)_{12}[\mathrm{M}_4\mathbf{1}_6]$	225 (-655); 242 (+1086); 290 (-216); 341 (-230); 375 (+330)	225 (-620); 242 (+1050); 289 (-197); 341(-225); 376 (+302)	225 (-583); 241 (+927); 292 (-212); 337 (-204); 371 (+267); 465 (-8); 560 (+7)
ΔΔΔΔ-$(\mathrm{NMe}_4)_{12}[\mathrm{M}_4\mathbf{1}_6]$	222 (+485); 241 (-870); 289 (+173); 338 (+194); 372 (-265)	n.d.	n.d.
ΛΛΛΛ-$(\mathrm{NMe}_4)_{12}[\mathrm{M}_4\mathbf{1}_6]$	223 (-473); 241 (+850); 288 (-179); 337 (-192); 373 (+267)	n.d.	n.d.

Samples concentrations were 0.5 mM and were prepared in 5 mM KOH solution. (n.d. = not determined)

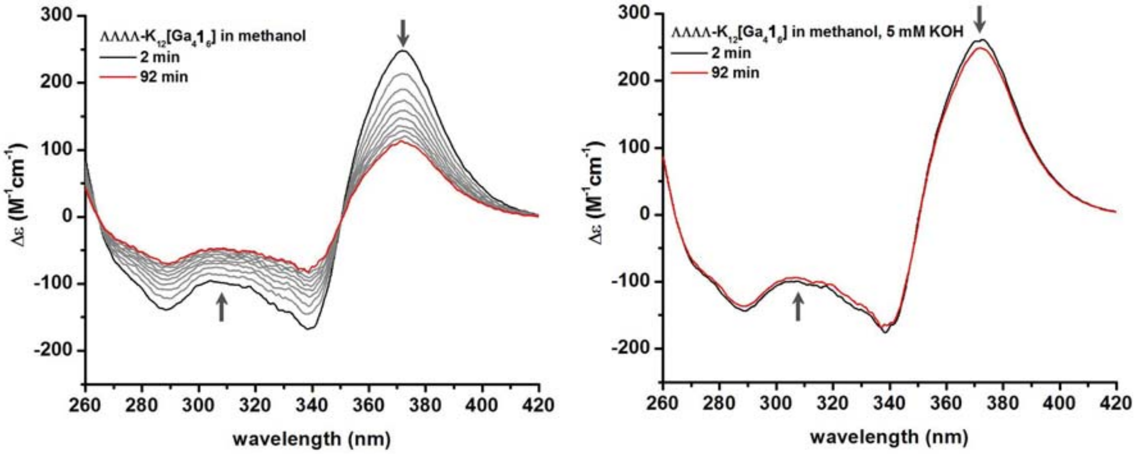

Figure 12. Left: CD spectra of $\Lambda\Lambda\Lambda\Lambda$-$K_{12}[Ga_4\mathbf{1}_6]$, monitored in MeOH at 10 min intervals. Right: CD spectra of $\Lambda\Lambda\Lambda\Lambda$-$K_{12}[Ga_4\mathbf{1}_6]$ in MeOH with 5 mM KOH. Spectra were recorded at 10 minute intervals.

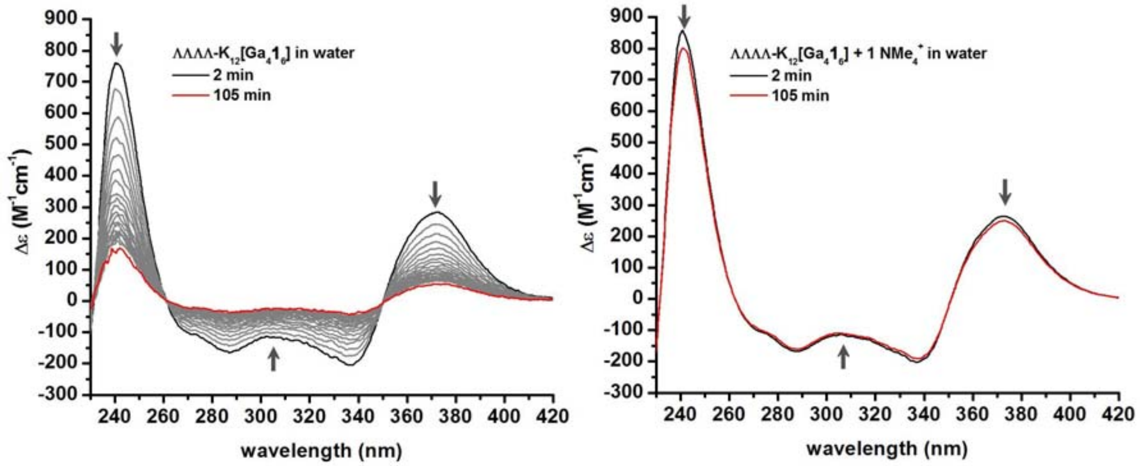

Figure 13. Left: CD spectra of $\Lambda\Lambda\Lambda\Lambda$-$K_{12}[Ga_4\mathbf{1}_6]$, monitored at neutral pH in H_2O. Spectra were taken in 5 minute intervals. Right: CD spectra of $\Lambda\Lambda\Lambda\Lambda$-$K_{12}[Ga_4\mathbf{1}_6]$ in the presence of one equivalent of NMe_4^+, monitored at neutral pH in H_2O.

SYNOPSIS TOC Figure: